Metastability of a granular surface in a spinning bucket

Chuck Yeung
Division of Science, Pennsylvania State University at Erie, The Behrend College, Erie, Pennsylvania 16536
(Received 28 October 1997)

The surface shape of a spinning bucket of granular material is studied using a continuum model of surface flow developed by Bouchaud *et al.* and Mehta *et al.* An experimentally observed central subcritical region is reproduced by the model. The subcritical region occurs when a metastable surface becomes unstable via a *nonlinear* instability mechanism. The nonlinear instability mechanism destabilizes the surface in large systems while a linear instability mechanism is relevant for smaller systems. The range of angles in which the granular surface is metastable vanishes with increasing system size. [S1063-651X(98)12504-7]

PACS number(s): 83.70.Dk, 46.10.+z, 46.30.−i, 47.20.−k

I. INTRODUCTION

Granular materials display very complex dynamics due to their both fluidlike and solidlike characteristics [1,2]. Even simple experiments can produce unexpected results. Examples are recent experiments in which measurements were taken of the granular surface of a bucket of sand spun about its cylindrical axis [3,4]. At low rotation rates a central region was observed in which the slope is significantly less than the critical slope [4–6]. This central subcritical region was conjectured to be due to the inertia of the flowing grains [4] since it could not be explained in terms of a simple theory, which assumed the surface was everywhere critical [7].

Many models have been developed to describe the evolution of a granular surface [8–15]. These models often assume that the flow is restricted to a thin layer of grains near the surface. Such models have been used extensively to study avalanches of a granular material in a horizontal rotating drum [16]. However, the spinning bucket experiment is a better testing ground for these ideas since, at least at low rotation rates, the fundamental assumption of a thin flowing layer is more likely to be true [17].

The purpose of this paper is twofold. The first is to apply the flow models to the spinning bucket experiment. The second is to explore the source and limits of the metastable behavior observed in the model. In particular, a continuum description of the surface flow developed by Bouchaud *et al.* [10] and Mehta *et al.* [11] is used. This model includes the effect of the inertia of the flowing grains and is known to exhibit metastability via a linear instability mechanism [10], i.e., the surface remains metastable for a range of angles beyond the minimum angle of repose. This difference in the minimum and maximum stable angles was argued to be the physical source of the Bagnold angle [10].

Here I show that this model qualitatively reproduces the central subcritical region. I determine the mechanism creating the subcritical region and show that it is closely intertwined with the metastability of the model. The metastable surface becomes unstable via a *nonlinear* instability, i.e., an instability to very small but noninfinitesimal perturbations. This nonlinear instability determines the dynamics for ''large'' systems while the linear instability is dominant for ''small'' systems. The range of metastable slopes and, hence the Bagnold angle, depends on the system size and vanishes in the limit of large systems.

II. SUMMARY OF EXPERIMENT

Figure 1 shows the setup for the spinning bucket experiment [3,4]. A bucket of radius R_0 is partially filled with common building sand. A conical pile is prepared at the angle of repose, $\theta_f = 34° \pm 1°$, by slowly dropping the plastic spheres onto the center of the stationary bucket. (Here we label the angle of repose θ_f since, in an ideal Coulomb material, the surface is everywhere critical and the angle of repose is the same as the angle of internal friction [1]). The rotation rate ω is then slowly increased until it reaches the desired value and the resulting surface shape is measured.

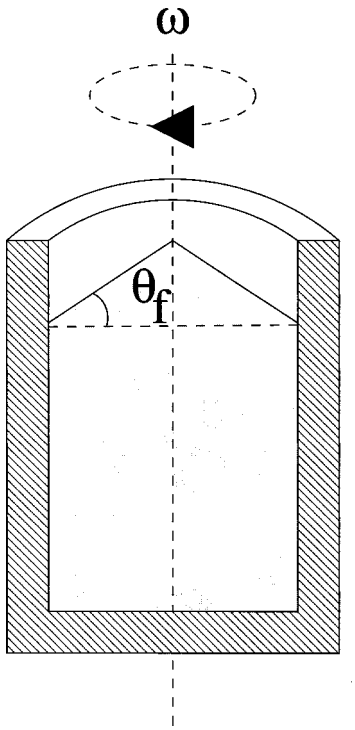

FIG. 1. A cut-away view of the spinning bucket experiment. A conical pile is prepared at the angle of repose θ_f. The cylinder is then spun about its vertical axis at rotation rate ω and the resulting surface shape is measured.

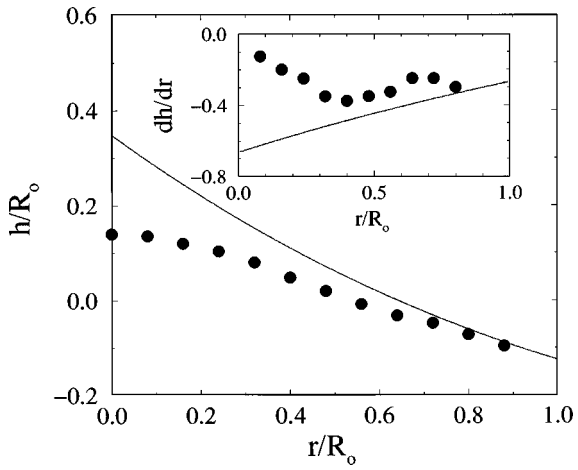

FIG. 2. The surface shape at $\Omega=\sqrt{\omega^2 R_0/g}=0.578$ as given in Ref. [4]. The center of the bucket is at $r=0$ and the edge at $r/R_0=1$. The dashed line is the result of an ideal Coulomb material with $\theta_f=34°$ and the points are the experimental data. The inset shows the experimental and theoretical slopes. The experiment and theory agree near the outer edge of the bucket but the slope at the center is significantly less negative than that of an ideal Coulomb material.

For an ideal Coulomb material the granular surface shape is found by assuming that the friction force is saturated and relating the net force on a surface element to the centripetal acceleration [3,4,6]. The critical slope S_- is a function of radial distance r and ω,

$$S^-(r)=\frac{dh}{dr}=\frac{(r/R_0)\Omega^2-\tan\theta_f}{1+(r/R_0)\Omega^2\tan\theta_f}, \tag{1}$$

where $h(r)$ is the local height, $\Omega=\sqrt{\omega^2 R_0/g}$ is the dimensionless rotation rate, g is the gravitational acceleration, and R_0 is the bucket radius. The $-$ superscript indicates that the friction force is inwards since the grains flow outwards. Note that $S^-(r)$ is negative for small Ω so that an unstable surface corresponds to $\partial h/\partial r<S^-(r)$.

Experimentally, the surface agrees well with Eq. (1) for intermediate rotation rates $2\lesssim\Omega\lesssim5$ [3,4] but less well for larger and smaller Ω. This paper will focus on the low rotation rates, $\Omega\lesssim2$. Figure 2 shows the experimental surface shape obtained by Baxter for $\Omega=0.578$ along with the prediction for a ideal Coulomb material using $\theta_f=34°$ [4]. The corresponding slopes are shown in the inset. There is reasonable agreement between experiment and theory at the outer edge ($r\gtrsim R_0/2$). However, in the center, $r\lesssim R_0/2$, the slope is much less than the critical slope. This was thought to be because the critical theory neglects the effects of grain inertia [4].

III. THE MODEL

To analyze the spinning bucket experiment we use a model of the granular surface evolution developed by Bouchaud *et al.* [10] and Mehta *et al.* [11]. The model assumes that all grains are stationary except for a thin layer of flowing grains on the top. We define $h(\mathbf{r},t)$ as the local height of the immobile pile and $\rho(\mathbf{r},t)$ as the thickness of the rolling layer. Here $\mathbf{r}$ is the two-dimensional vector giving the projection of the local position onto the x-y plane.

The dynamics of the rolling layer $\rho(\mathbf{r},t)$ is given by

$$\frac{\partial\rho}{\partial t}=-\nabla\cdot(\mathbf{v}\rho)+D_0\nabla^2\rho+\Gamma_0(\{h\},\{\rho\}), \tag{2}$$

where $\mathbf{v}=v_0\hat{\mathbf{r}}$ is the local velocity of the rolling layer, D_0 is the diffusion constant, and Γ_0 is the rate of conversion from immobile to mobile grains and ∇ and ∇^2 are the two-dimensional gradient and Laplacian, respectively. Assuming that the grains flow outward, the conversion rate is

$$\Gamma_0(\{h\},\{\rho\})=-\rho\left[\gamma_0\left(\frac{\partial h}{\partial r}-S^-(r)\right)+\kappa_0\nabla^2 h\right]-\alpha_0\left[\frac{\partial h}{\partial r}-S^-(r)\right]\mathcal{H}\left(\frac{\partial h}{\partial r}-S^-(r)\right), \tag{3}$$

where $\mathcal{H}$ is the Heaviside function. The first term in Γ_0 accounts for the conversion of static grains to rolling grains when the slope is steeper than the critical slope ($\partial h/\partial r<S^-$) and vice versa for a shallower slope. The $\rho\kappa_0\nabla^2 h$ term causes valleys to fill and peaks to smooth. The last term in Γ_0 accounts for the jarring loose of static grains by the rotation of the bucket even in the absence of a flowing layer. Finally, assuming that bulk rearrangement of material can be neglected, conservation of total material requires

$$\frac{\partial h}{\partial t}=-\Gamma_0(\{h\},\{\rho\}). \tag{4}$$

For $\alpha_0=0$ the model is the same as that introduced by Bouchaud *et al.* [10]. Mehta *et al.* allowed for a nonzero α_0 and also included an additional bulk arrangement term [11].

To compare with experiment we require a rough estimate of the model parameters:

(i) The speed of the rolling grains v_0 can be estimated from the speed of a grain falling through a grain diameter d_0: $v_0\approx\sqrt{2gd_0}$.

(ii) A narrow bump of rolling grains starting at the center will reach the edge of the bucket in time $t_0=R_0/v_0$. Diffusion causes this bump to spread to a width $\Delta x=\sqrt{D_0 t_0}=\sqrt{D_0 R_0/v_0}$ when it reaches the edge. Since $\Delta x\sim\sqrt{R_0}$ the width of the bump is much less than the system size for large R_0. Therefore the ''large'' system limit corresponds to

$$\frac{(\Delta x)^2}{R_0^2}=\frac{D_0}{v_0 R_0}\ll1. \tag{5}$$

The ''small'' limit corresponds to the width of the bump being of the same order as the system or $D_0/(v_0 R)\gtrsim1$ [18].

(iii) $\gamma_0\Delta S d_0/v_0$ is the probability that a rolling grain jars loose a static grain as it rolls over it. A typical excess slope of $\Delta S=0.1$ and, assuming a 10% probability that the static grain is converted to rolling, gives $\gamma_0\approx v_0/d_0$.

(iv) The ratio κ_0/γ_0 defines a length scale on which the hole filling–peak smoothing mechanism dominates. This is important only at very small length scales on the order of a few grain diameters so $\kappa_0\approx d_0\gamma_0$.

(v) α_0 depends on the noise in the apparatus. The generation of rolling material by noise is assumed to be much less effective than the convection so that $\alpha_0 \ll v_0$.

Equations (2)–(4) can be rewritten in dimensionless form by measuring lengths in terms of the bucket radius R_0 and time in terms of $t_0 = R_0/v_0$,

$$\frac{\partial \rho}{\partial t} = -\nabla\cdot(\hat{\mathbf{r}}\rho) + D\nabla^2\rho + \Gamma(\{h\},\{\rho\}), \tag{6}$$

where

$$\Gamma(\{h\},\{\rho\}) = -\rho\left[\gamma\left(\frac{\partial h}{\partial r} - S^-(r)\right) + \kappa\nabla^2 h\right] - \alpha\left[\frac{\partial h}{\partial r} - S^-(r)\right]\mathcal{H}\left(\frac{\partial h}{\partial r} - S^-(r)\right), \tag{7}$$

and

$$\frac{\partial h}{\partial t} = -\Gamma(\{h\},\{\rho\}). \tag{8}$$

The dimensionless parameters are $D = D_0/(v_0 R)$, $\gamma = \gamma_0 R/v_0$, $\kappa = \kappa_0/v_0$ and $\alpha = \alpha_0/v_0$.

Assuming a large system, order of magnitude estimates of the dimensionless parameters can be obtained from the earlier estimates:

$$D \equiv \frac{D_0}{v_0 R} \ll 1, \gamma \equiv \frac{\gamma_0 R}{v_0} \approx \frac{R}{d_0},$$

$$\kappa \equiv \frac{\kappa_0}{v_0} \approx \frac{d_0}{R}\gamma, \quad \alpha \equiv \frac{\alpha_0}{v_0} \ll 1. \tag{9}$$

The speed of the rolling layer is unity under this rescaling. As shown in the next section, the behavior of the model is most sensitive to γ and less sensitive to the exact value of D and κ as long as $D \ll 1$ and $\kappa/\gamma \ll 1$.

An especially interesting feature of this model is that it displays metastability and hysteresis. Bouchaud *et al.* performed a linear stability analysis by balancing the rate at which a small bump of the rolling layer is convected downhill with the rate at which the bump is amplified and diffuses [10]. They found that the bump affects the behavior uphill only if the slope exceeds the critical slope by an amount larger than

$$\Delta S = S^- - \frac{\partial h}{\partial r} > \frac{v_0^2}{D_0\gamma_0} = \frac{1}{D\gamma}. \tag{10}$$

The metastable behavior was interpreted as the physical source of the Bagnold angle, i.e., the excess angle beyond the angle of repose at which a static sandpile first becomes unstable. This dynamical interpretation of the Bagnold angle is very different from the usual mechanical interpretation of this angle [10].

IV. NUMERICAL RESULTS

A. Spinning bucket

To analyze the spinning bucket experiment, Eqs. (6)–(8) were numerically integrated in polar coordinates with azimuthal symmetry. Using the experimental parameters, $\theta_f = 34°$, $d_0 \approx 0.25$ mm and $R_0 = 12.5$ cm [4], we obtain $\gamma = R_0/d_0 = 500$ and $\kappa/\gamma = d_0/R_0 = 1/200$. Assuming a ''large'' system and small vibrations, we choose $D = 0.001 \ll 1$ and $\alpha = 10^{-8}$. A third-order Adam-Bashford method was used [19] with mesh-size $\delta x = 0.002$ and time-step $\delta t = 5\times 10^{-7}$. Zero slope boundary conditions are applied at $r = 0$ and zero curvature boundary conditions at $r = 1$. Any rolling material reaching the edge is converted to static.

An initial conical pile is prepared at the critical angle and the rotation rate Ω is increased instantaneously from $\Omega = 0$ to $\Omega = 0.6$. Since the critical slope decreases with Ω the initial surface is unstable and, as shown in Fig. 3, an avalanche is generated. At $t \approx 0.125$ [Fig. 3(a)] a buildup of flowing material is visible at the edge of the bucket. This buildup generates a steep local slope in the static pile that causes the static material uphill to fail. The failure then propagates uphill, reaching the center of the bucket at $t \approx 0.2$ [Fig. 3(b)]. The static pile beneath the flowing layer approximately follows the critical curve. The flowing layer then convects to the edge of bucket [Fig. 3(c)] leaving behind a central subcritical region in which the slope is much less than the critical slope [Fig. 3(d)].

The integration was repeated with different values of D, γ, and κ to test the robustness of the results. The central subcritical region is qualitatively the same for all $\gamma \gtrsim 400$ and $D \lesssim 0.005$, becoming more pronounced for larger γ and smaller D. For smaller γ and larger D ($\gamma \lesssim 200$ and $D \gtrsim 0.02$) the final surface follows closely the critical surface. Varying the ratio κ/γ or α did not have noticeable effect as long as they were small but nonzero.

A comparison of model results in Fig. 3 with the experimental data in Fig. 2 shows that the essential features of the experiment are reproduced. In particular, there is a subcritical region in the center and a region near the edge that follows the critical surface. However, a more detailed analysis shows two important differences. First, the flowing layer is much larger than the few grains assumed in the model. Second, in the experiment, the rotation rate is slowly ramped up from zero rather than changed instantaneously. Hence the numerical results correspond to the actual experiment only if the final surface is independent of the initial state, or, if the initial conical surface is metastable up to an Ω close to 0.6.

To mimic the experiment more closely we repeat the integration while slowly ramping the rotation rate from $\Omega = 0$ to $\Omega = 0.6$. We monitor the excess slope before an avalanche occurs, i.e., the amount the slope of the metastable surface exceeds the critical slope, and the magnitude of the subcritical region after an avalanche, i.e., the amount the slope of static surface falls below the critical slope.

The conical surface is metastable as Ω is increased from zero until the first avalanche occurs at $\Omega \approx 0.2$. The dynamics of this avalanche is very similar to that for the instantaneous jump to $\Omega = 0.6$. The main differences are that the excess slope before and the magnitude of the static slope after the avalanche are both much smaller for the instantaneous jump

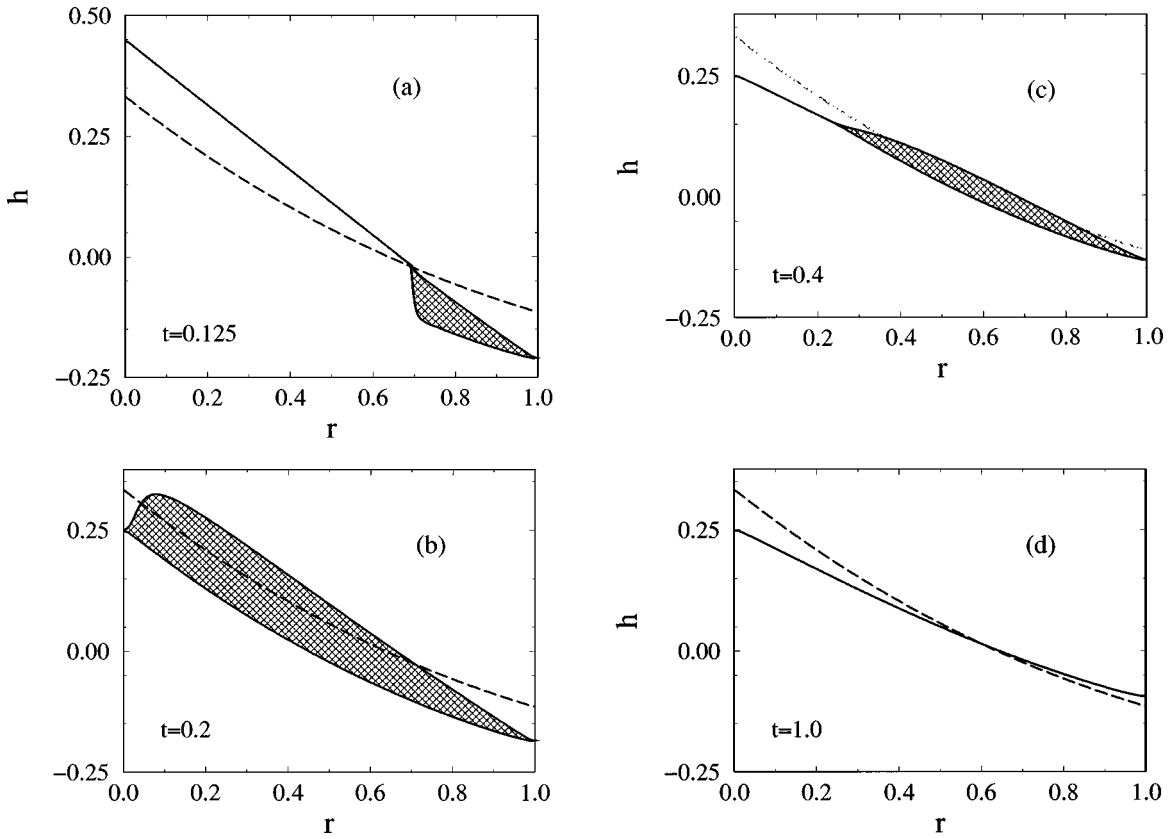

FIG. 3. The evolution of a conical pile at $\Omega = 0.6$. The dashed line is the critical surface and the shaded area is the flowing layer. In (a) a flowing region has formed at the edge of the bucket. This failure zone propagates uphill, reaching the center in (b). The static surface under the flowing layer closely follows the critical surface. The flowing layer convects downhill (c) and the final surface (d) has a central region with a slope less than the critical slope.

to $\Omega = 0.6$. As Ω is increased further the critical slope decreases and becomes shallower than the new static slope. Eventually a second avalanche occurs at $\Omega \approx 0.35$. The process repeats, leading to a third avalanche at $\Omega \approx 0.45$ and a fourth at $\Omega \approx 0.55$. After each avalanche a subcritical region is observed with a much smaller magnitude than for the instantaneous jump. This indicates that the magnitude of the subcritical region after an avalanche increases with the excess slope before the avalanche. This was confirmed by instantaneously changing the rotation rate to different values of Ω and observing the subcritical region after the resulting avalanches.

B. Two-dimensional sandpile

The numerical results indicate that the central subcritical region is closely related to the metastable behavior of the model. To understand the factors determining the limits of metastability we consider the simpler case of a two-dimensional sandpile in a stationary container ($\Omega = 0$ and $\alpha = 0$). This eliminates the complications of the cylindrical geometry and the constant production of flowing grains by the bucket rotation.

We start by preparing a static critical surface. We first produce a surface at the critical slope $\partial h/\partial x = -\tan\theta_f$ along with a small uniform rolling layer. Here x is the linear position measured in units of the system size L_0 with the high end of the pile at $x = 0$ and the low end at $x = 1$. This constant slope surface is not stationary due to the finite value of κ. To obtain the static critical surface we integrate Eqs. (6)–(8) in one dimension until the initial flowing layer is completely converted to static.

Once this static critical surface is obtained, we destabilize it by tilting the surface through an excess slope ΔS. We also assume the tilt produces a uniform flowing layer $\Delta\rho$. To determine the characteristics of the resulting avalanche, we used a large $\Delta S = 0.1$ with the same parameters as we used for the spinning bucket $\gamma = 500$, $D = 0.001$, $\kappa/\gamma = 1/500$ and $\Delta\rho = 10^{-8}$. The mesh size was $\delta x = 0.001$ and time step $\delta t = 2 \times 10^{-7}$. The resulting avalanche has the same features as the avalanche in the spinning bucket:

(1) The avalanche is induced by the growth of the rolling layer at the foot of the pile.

(2) This buildup of the rolling layer creates a valley in the static pile. The large local slope of the static pile causes the static material uphill to fail.

(3) The failure zone propagates uphill until it reaches the top of the pile. As shown in Fig. 4, the surface of the static pile below the rolling layer follows closely the critical surface. However, a more detailed examination (inset of Fig. 4) shows that the surface of the static pile is slightly less steep than the critical slope.

(4) Since the propagation of the failure zone is faster than the convection of grains down the hill, the total height of the pile (static+flowing) is the same as the initial static pile.

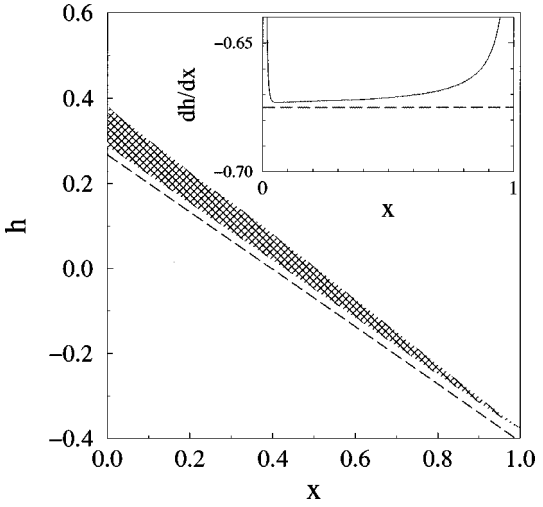

FIG. 4. The two-dimensional sandpile immediately after the failure zone has propagated all the way to the top. The static layer below the rolling layer follows closely the critical slope (dashed line). However, as shown in the inset, the slope of the static layer (solid line) is slightly less steep than the critical slope (dashed line).

Therefore, the built-up flowing layer at t^*, the time the failure zone reaches the top of the hill, is

$$\rho(x,t^*) \approx h(x,0) - h(x,t^*) = \Delta S(1-x).$$

This is confirmed in Fig. 4, which shows a triangular shaped flowing layer with $\rho(0,t^*) = \Delta S$ and $\rho(1,t^*) = 0$.

(5) The rolling layer flows downhill leaving a subcritical region at $x < 0.5$. The surface for $x \gg 0.5$ follows closely the critical surface except at the very edge where there is a buildup of the static pile [13].

Since the magnitude of the subcritical region after an avalanche depends on the excess slope before, we need to explore the limits of metastability. The linear stability analysis predicts that the surface is stable until the excess slope exceeds $\Delta S^* = 1/(D\gamma)$ [10]. However, several characteristics of the avalanche indicate that a different mechanism may destabilize the surface. First, the instability always begins at the bottom of the pile, indicating that the system size is important. Second, the avalanche is generated when there is an increase in the local steepness of the static pile. The linear stability analysis neglects the effect of the flowing layer on the static pile.

To check if the linear stability dominates the dynamics, we determined ΔS^*, the minimum excess slope required to initialize an avalanche, as a function of the different parameters. Figure 5(a) shows ΔS^* as a function of the amplification rate γ. Although both the linear stability prediction and the observed ΔS^* are proportional to $1/\gamma$, the observed values are a factor of 20 smaller than the linear prediction.

A more serious conflict is shown in Fig. 5(b) where ΔS^* is plotted as a function of D. The numerical results clearly deviate from the linear stability prediction that $\Delta S^* \propto 1/D$ for small D. Hence, for large systems, i.e., small D, the linear stability mechanism is not relevant to the surface evolution in this limit. On the other hand, for large D, $\Delta S^* \sim 1/D$ so the linear instability mechanism may be relevant for small

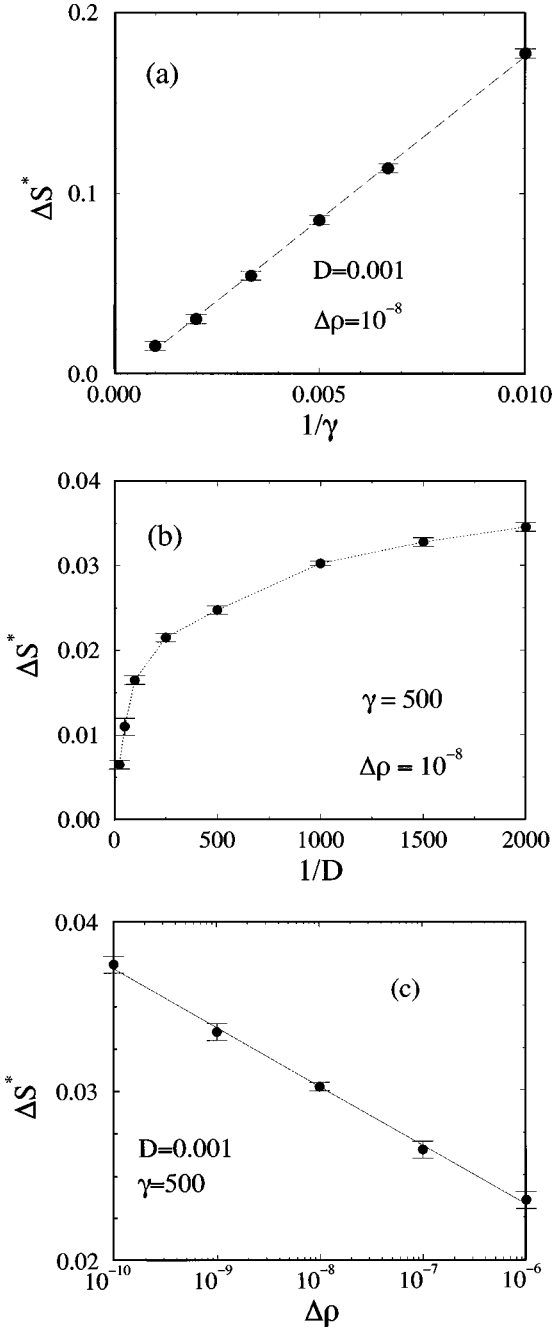

FIG. 5. (a) The critical excess slope ΔS^* as a function of $1/\gamma$. The dashed line is a straight line fit showing that $\Delta S \sim 1/\gamma$. (b) $\Delta S a^*$ as a function of $1/D$. For small D (or large systems) ΔS is only weakly dependent on D. For large D, $\Delta S^* \sim 1/D$ indicating the linear instability may initialize the avalanches in small systems. (c) ΔS^* as a function of the initial rolling layer $\Delta\rho$. The dashed line is a straight line fit showing that $\Delta S \sim -\ln(\Delta\rho)$.

systems. However, for large D, the subcritical region disappears and the final state follows closely the critical surface.

Figure 5(c) shows ΔS as a function of the rolling layer $\Delta\rho$. Here $\Delta S^* \propto -\ln(\Delta\rho)$ so that the metastability of the initial granular surface depends on the amplitude of the initial perturbation. In particular, a small but noninfinitesimal rolling layer is required to induce an avalanche, indicating that the avalanche is initiated through a nonlinear instability mechanism.

V. THEORY AND ANALYSIS

A. Nonlinear instability mechanism

To understand the metastable behavior observed numerically two effects must be considered: First, the flowing layer is amplified as it flows downhill, and second, the amplification of the flowing layer changes the slope of the static pile.

To do so we modify an argument given by Bouchaud *et al.* for the amplification of a bump of rolling grain as it flows [10]. Consider a critical surface tilted through an initial excess slope ΔS with an uniform flowing layer $\Delta\rho$. Neglecting any change in the static pile, Eq. (6) shows that the flowing layer will grow exponentially as it flows downhill. For small D, the flowing layer will approximately maintain its shape so

$$\rho(x,t)\approx\begin{cases}0 & \text{if } x<t,\\ \Delta\rho e^{\gamma\Delta S t} & \text{if } x>t.\end{cases} \tag{11}$$

In terms of the dimensionless variables both the radius of the bucket and the speed of the grains is unity. Therefore for $t>1$ all flowing material reaches the bottom, leaving the origin static state intact.

This argument indicates that the granular surface is stable for all ΔS. However, this is the case only if the change in the static pile can be neglected. The change in $h(x,t)$ for small D is

$$\Delta h(x,t)\equiv h(x,t)-h(x,0)=-\int_0^t dt'\,\Gamma(\{h\},\{\rho\})$$

$$\approx-\int_0^t dt'\,\gamma\Delta S\rho(t'). \tag{12}$$

Substituting Eq. (11) for $\rho(t')$ and integrating to $t>1$ gives [since $\rho(x,t)=0$ if $t>x$]

$$\Delta h(x,t)=-\Delta\rho(e^{\gamma\Delta S x}-1), \tag{13}$$

Therefore the flowing layer generates an additional excess slope of

$$\Delta S'(x)=-\frac{d\Delta h}{dx}=\gamma\Delta S\Delta\rho e^{\gamma\Delta S x}. \tag{14}$$

If $\Delta S'$ is not small there will be a positive feedback mechanism. The increased steepness makes the flowing layer grow faster, which in turn generates an even larger excess slope. Once this positive feedback mechanism builds up, the increased slope causes the material uphill to fail and the failure zone propagates up to the top of the hill. Since $\Delta S'(x)$ is largest at $x=1$ the avalanche must start at the bottom of the pile in agreement with numerical observations.

Using Eq. (14) the minimum initial excess angle required for an avalanche occurs when $\Delta S'(1)\approx 1$ or $\gamma\Delta S^*\Delta\rho e^{\gamma\Delta S^*}\approx 1$. Solving for ΔS^* gives

$$\Delta S^*\approx-\frac{\ln(\Delta\rho)+\ln(\gamma\Delta S^*)}{\gamma}\approx-\frac{\ln\Delta\rho}{\gamma}, \tag{15}$$

where we assume $\Delta\rho\ll 1$. This result is in agreement with our numerical results of the previous section: $\Delta S^*\sim 1/\gamma$, $\Delta S^*\sim-\ln(\Delta\rho)$ and ΔS^* approximately independent of D for small D.

A more intuitive understanding is obtained by rewriting the metastability criteria in terms of the original unscaled parameters. Using $\gamma=\gamma_0 L_0/v_0$ and $\Delta\rho=\Delta\rho_0/L_0$ to rewrite Eq. (15) in terms of the dimensionful variables we have

$$\Delta S^*\approx-\frac{v_0}{\gamma_0 L_0}\ln\left(\frac{\Delta\rho_0}{L_0}\right). \tag{16}$$

Therefore, according to this model, the range of metastable slopes and hence, the Bagnold angle, depends on the system size L_0. Furthermore ΔS^* vanishes as $L_0\to\infty$ showing that the metastability vanishes for infinite systems. This is because it takes time $t_0=L_0/v_0$ for the flowing material at the top of the hill to reach the bottom. During this time the flowing layer is amplified by a factor $e^{\gamma_0\Delta S\, t_0}$. The larger the system the more the flowing layer is amplified and the more likely an avalanche is initiated.

B. Central subcritical region

We now return to the origin of the central subcritical region observed after an avalanche. Assume an avalanche is initiated at the bottom of the pile. For large γ and small D, we empirically find that failure zone propagates uphill much faster than the rate at which grains are convected downwards. We find that the static pile below the flowing layer is slightly less steep than the critical surface (see Fig. 4). Since the slope of the static pile is less than critical, the built-up rolling layer is continually converted to static as the layer flows down the hill. The flowing layer is convected away from the top of the pile first so this conversion occurs longest at the bottom, leading to final surface that is shallower than the critical surface.

This argument can be made more quantitative by approximating the built-up rolling layer as a constant $\rho(x,t_1)=\Delta S$ where t_1 is the time the failure zone reaches the top of the pile. As a further approximation, we also assume that the underlying static pile has a constant slope slightly less steep than critical $\partial h/\partial x=-\tan\theta_f+S_D$ where S_D is the deviation of the static pile from the critical slope. For small D we can neglect the change in the shape of the flowing layer as it is convected downhill:

$$\rho(x,t)=\begin{cases}0 & \text{if } t-t_1>x\\ \Delta S e^{-\gamma\Delta S t} & \text{if } t-t_1>x.\end{cases} \tag{17}$$

The change in the static pile after the flowing layer has passed is

$$\Delta h(x,t)=-\int_{t_1}^t dt'\,\Gamma(\{h\},\{\rho\})=\int_{t_1}^t dt'\,\gamma S_D\rho(x,t'). \tag{18}$$

Substituting Eq. (17) for $\rho(t')$ and integrating to $t-t_1>1$ gives the total change in h,

$$\Delta h(x)=\Delta S(1-e^{-\gamma S_D x}). \tag{19}$$

Therefore the slope of the static pile after the avalanche is

$$\frac{\partial h}{\partial x} = -\tan\ \theta_f + S_D + \frac{\partial \Delta h}{\partial x} = -\tan\theta_f + S_D + \gamma S_D \Delta S e^{-\gamma S_D x}$$

$$\approx -\tan\theta_f + \gamma S_D \Delta S e^{-\gamma S_D x}, \tag{20}$$

where we neglect the second term since γ is large. This result is in agreement with our qualitative picture. In particular, the deviation of the static pile from the critical surface is largest at small x.

VI. SUMMARY

We have applied a model of granular surface flow developed by Bouchaud *et al.* [10] and Mehta *et al.* [11] to the spinning bucket experiments of Baxter [3,4]. The model qualitatively reproduces the central subcritical region observed in the experiment at low rotation rates. The subcritical region occurs when a metastable surface becomes unstable via a *nonlinear* instability mechanism. The nonlinear instability is due to the amplification of the rolling layer as it is convected downhill. This amplified layer causes the static pile underneath to become steeper, which in turn causes the flowing layer to become even larger. This positive feedback mechanism initiates the avalanches in ''large'' systems. We numerically determined the excess slope required to destabilize the metastable surface as a function of system parameters and showed that it agrees with our analytic arguments. In particular, the model predicts that the excess slope, and hence the Bagnold angle, depends on system size and vanishes in the limit of large systems. Lastly we showed how the nonlinear instability leads to the central subcritical region via a conversion of rolling grains to static as they roll downhill.

ACKNOWLEDGMENTS

I thank G.W. Baxter for many useful discussions and comments and for providing the experimental data in Fig. 2. I am grateful to Ron McCarty for providing some of the computational resources. This work was supported by Cottrell College Science Grant No. CC3993 from the Research Corporation.

[1] R. M. Nedderman, *Statics and Kinetics of Granular Materials* (Cambridge University Press, Cambridge, UK, 1992).
[2] For reviews, see H. M. Jaeger and S. R. Nagel, Science **255**, 1523 (1992); H. M. Jaeger, S. R. Nagel, and R. P. Behringer, Phys. Today **49**(4), 32 (1996); H. M. Jaeger, S. R. Nagel, and R. P. Behringer, Rev. Mod. Phys. **68**, 1259 (1996).
[3] M. Vavrek and G. W. Baxter, Phys. Rev. E **50**, 3353 (1994).
[4] G. W. Baxter (unpublished).
[5] Variations from the critical surface were also observed in a similar experiment by Medina *et al.* [6] although in this case, the variation was interpreted to be due to fluctuations in the angle of repose.
[6] A. Medina, E. Luna, R. Alvarado, and C. Trevino, Phys. Rev. E **51**, 4621 (1995).
[7] See, for example, *Statics and Kinetics of Granular Materials* (Ref. [1]), Chap. 3.
[8] T. A. J. Duke, G. C. Barber, and A. Mehta, Europhys. Lett. **13**, 19 (1990).
[9] H. F. Ouyang, Y. N. Lu, and E. J. Ding, Phys. Rev. E **48**, 2413 (1993).
[10] J. P. Bouchaud, M. E. Cates, J. R. Prakash, and S. F. Edwards, Phys. Rev. Lett. **74**, 1982 (1995); J. P. Bouchaud, M. E. Cates, J. R. Prakash, and S. F. Edwards, J. Phys. I (France) **4**, 1383 (1994).
[11] A. Mehta, in *Granular Matter*, edited by A. Mehta (Springer-Verlag, Berlin, 1994); A. Mehta, J. M. Luck, and R. J. Needs, Phys. Rev. E **53**, 92 (1996).
[12] G. C. Barker and A. Mehta, Phys. Rev. E **53**, 5704 (1996).
[13] T. Boutreaux and P. G. de Gennes, J. Phys. I (France) **6**, 1295 (1996).
[14] H. A. Makse, P. Cizeau, and H. E. Stanley, Phys. Rev. Lett. **78**, 3298 (1997).
[15] D. A. Head and G. J. Rodgers (unpublished).
[16] H. M. Jaeger, C.-H. Liu, and S. R. Nagel, Phys. Rev. Lett. **62**, 40 (1989).
[17] For example, Barker and Mehta have argued that the rotating drum experiment is dominated by local rearrangement of grains rather than macroscopic flow [12].
[18] These limits were discussed in Ref. [10] in terms of a Peclét number $(v_0 R)/D_0$ was called the Peclét number in Ref. [10].
[19] W. H. Press, S. A. Teukolsky, W. T. Vetterling, and B. P. Flannery, *Numerical Recipes in C: The Art of Scientific Computing* (Cambridge University Press, Cambridge, UK, 1992).